International Journal of
Translational Medicine

MDPI

Communication

Cell Responses to Simulated Microgravity and Hydrodynamic Stress Can Be Distinguished by Comparative Transcriptomics

Nik V. Kouznetsov

Karolinska Institutet, Nobels väg 16, 171 77 Stockholm, Sweden; nikkuznetsov@inbox.com

Abstract: The human immune system is compromised in microgravity (MG) conditions during an orbital flight and upon return to Earth. T cells are critical for the immune response and execute their functions via actin-mediated immune cell-cell interactions that could be disturbed by MG conditions. In our study, we have applied two conventional platforms to simulate MG conditions: fast rotating clinostat (CL) and random positioning machine (RPM), followed by global T cell transcriptome analysis using RNA sequencing. Noteworthily, both selected rotational simulated MG platforms employ forced cell movement in cultural medium and expose cells to shear forces, therefore inducing certain cell response to hydrodynamic stress. We demonstrate that the T cell transcriptome profile in response to simulated MG treatment was clearly distinguishable from the T cell transcriptome response to hydrodynamic stress (HS). Gene expression profiling of genes related to or involved in actin cytoskeleton networks using RT-qPCR confirmed two sets of differentially regulated genes in the T cell response to MG or to HS. Several key genes potentially involved in T cell gravisensing (*Fam163b*, *Dnph1*, *Trim34*, *Upk-1b*) were identified. A number of candidate biomarker genes of the response to MG (*VAV1*, *VAV2*, *VAV3*, and *NFATC2*) and of the response to HS (*ITGAL*, *ITGB1*, *ITGB2*, *RAC1*, and *RAC2*) could be used to distinguish between these processes on the gene transcription level. Together, MG induces changes in the overall transcriptome of T cells, leading to specific shifts in the expression of cytoskeletal network genes.

Keywords: microgravity; hydrodynamic stress; transcriptome; actin cytoskeleton; gene expression

check for updates

Citation: Kouznetsov, N.V. Cell Responses to Simulated Microgravity and Hydrodynamic Stress Can Be Distinguished by Comparative Transcriptomics. *Int. J. Transl. Med.* **2022**, 2, 364–386. https://doi.org/10.3390/ijtm2030029

Academic Editor: Pier Paolo Claudio

Received: 18 May 2022
Accepted: 20 July 2022
Published: 25 July 2022

Publisher's Note: MDPI stays neutral with regard to jurisdictional claims in published maps and institutional affiliations.

Copyright: © 2022 by the author. Licensee MDPI, Basel, Switzerland. This article is an open access article distributed under the terms and conditions of the Creative Commons Attribution (CC BY) license (https://creativecommons.org/licenses/by/4.0/).

1. Introduction

The discovery of pressure and temperature receptors in vertebrates was recently recognized by being awarded the Nobel Prize 2021. Another physiological response to the environment, namely, the mechanisms underlying cell gravity sensing, remains largely unknown. In this regard, the nature of gravitational sensor structures or mechanisms that respond to gravity change in cells, for example, in lymphocytes, is still to be determined.

T cells need to rearrange their actin cytoskeleton for proper activation of the immune response [1]. The actin cytoskeleton proteins are putative candidates to participate in gravitational sensing [2,3]. Microgravity induces the repression of T cell-mediated immune response. Particularly, the T cell response towards mitogens in astronauts is reduced after space flight [2]. Human T cells stimulated with the mitogen concanavalin A reveal considerably reduced in vitro activation and cell proliferation in microgravity [2] and on a sounding rocket flight [4]. Stimulated T cells, pre-exposed to microgravity, show decreased expression of activation receptors, including CD25, CD69, and CD71, and reduced inflammatory cytokine secretion and cell proliferation when compared to T cells under normal gravity [5]. Moreover, human lymphocytes undergo apoptosis upon exposure to modelled low gravity [6]. The inhibition of lymphocyte proliferation in microgravity is due to alterations occurring within the first hours of exposure to microgravity [7,8]. Microarray expression analysis reveal changes in cytoskeletal gene expression [9] and overall altered patterns of global gene expression in space flown

human T cells when compared to T cells activated in 1 g control for normal gravity during space flight [10,11]. Impaired induction of early genes, regulated by transcription factors NF-κB, CREB, ELK, AP-1 and STAT, contributed to T cell inhibition in artificial low gravity [12]. Analysis of gene expression in T cells from four astronauts on board the ISS identified 99 down-regulated genes in microgravity, showing that expression of many important proinflammatory cytokines and chemokines was inhibited. Among them, 47 genes most significantly down-regulated in MG after 1.5 h, demonstrating inhibition of key immediate early genes (IEGs) [10]. In the context of cytoskeletal regulation, it was especially interesting that a majority of the genes that were inhibited in T cells in microgravity contained DNA serum response elements (SRE) in the promoters that bind the serum response factor (SRF) [10] as a part of transcriptionally active SRF/MRTFA complex. The SRF/MRTFA plays a key role in actin cytoskeleton organization by targeting the transcription of genes encoding cytoskeletal proteins and is involved in several processes, including cell growth and motility, apoptosis, and cancer progression [13–15].

To explore changes in gene regulation of T cells under simulated microgravity during longer time points, we have applied the well-established microgravity simulation platforms. We compared T cells for 8 and 24 h using clinostat (CL) and the random positioning machine (RPM) as key experimental systems [16] to simulate microgravity for suspension cell cultures (Figures 1A and A1). Both simulated MG (SMG) platforms employ forced cell movement in a cultural media, therefore, cell response to the hydrodynamic stress (HS) induced by shear forces during cell movement in liquid had to be taken into account as well. We demonstrate that simulated microgravity affects T cell gene expression, particularly the expression of actin cytoskeleton networks genes. SMG conditions induce shifts in the T cell transcriptome landscape that can be clearly distinguished from characteristic transcriptome profile caused by HS-only inducing rotational platform control treatment. Several regulatory key genes potentially acting as components of T cell gravitation sensory pathways and a number of candidate marker genes of the responses to MG and to HS were identified. Altogether, our transcriptomics-based approach allowed us to compare and discriminate two types of T cell response and to reveal a new set of genes involved in the response to simulated microgravity.

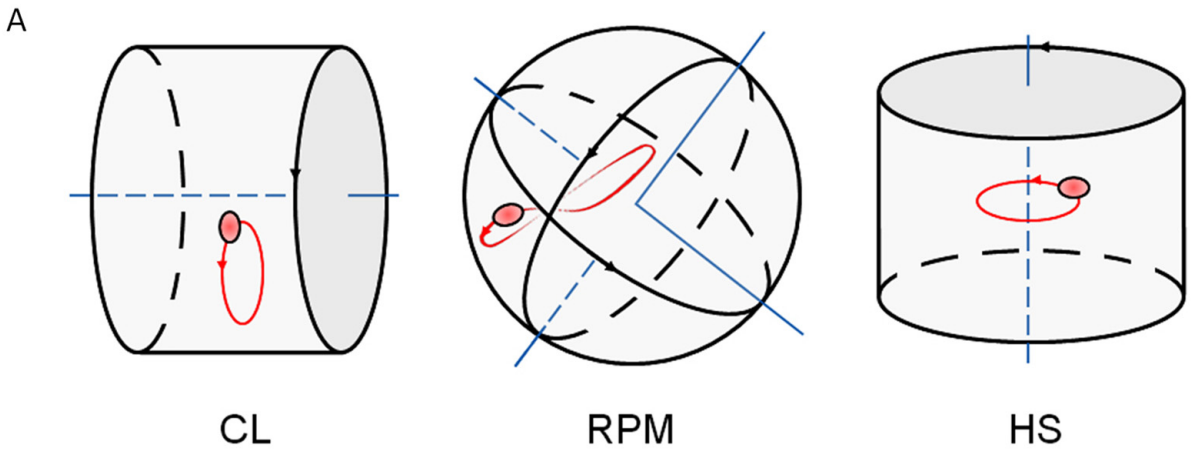

Figure 1. *Cont.*

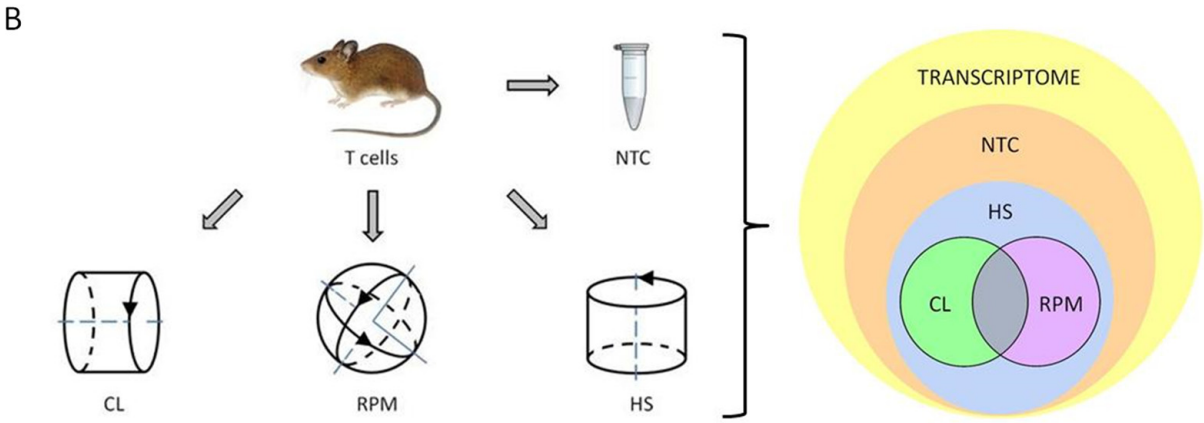

Figure 1. The principle and settings of experiment. (**A**) **The principle of simulated microgravity experiments performed with mouse primary T cells (thymocytes) and human T cell culture (Jurkat) samples.** Fast rotating clinostat (CL) and random positioning machine (RPM) used as simulated microgravity platforms. When rotating at sufficient speed, the suspension culture cells will be distributed homogeneously because the directional response to gravity is cancelled out. The cells rotate about themselves in simulated microgravity around one axis in CL and move randomly around two axes in RPM. Orbital shaker used as a hydrodynamic cell stress-inducing platform (HS). Direction of platform rotation is indicated by black arrows. Cell suspension sample movement illustrated by exemplary single cell trajectory shown in red. (**B**) **The overview chart of experiment settings and output of RNA-seq transcriptome data analysis**. Cell suspension of isolated primary mouse thymocytes (mouse T cells) was split into four parts, with each part treated as indicated. All four parts were processed for RNA isolation and generation of RNA library followed by RNA sequencing. The output sequencing results showed that most of RNA transcripts of mouse T cell transcriptome were detected in SMG-treated samples as well as in non-treated control (NTC) sample. Mouse T cell transcriptome response to microgravity in each of the used experimental platforms -clinostat (CL) and random positioning machine (RPM) develops in parallel with and mainly on a transcriptional background of T cell response to hydrodynamic stress (HS). The transcripts overlapping between CL and RPM panels were considered to represent gene candidates of the specific mouse T cell transcriptome response to simulated microgravity.

2. Materials and Methods

2.1. Mouse Primary T Cells Isolation

Primary thymocytes (mouse T cells) were isolated from thymi of three wt *C57BL/6* male mice at 10 weeks of age as sources for biological triplicates. Thymi were homogenized through 100 µm strainers (Corning, NY, USA) and cells were resuspended in sterile 1 × PBS. In cell counting with a hemocytometer, the consistent measurements of one biological sample performed twice were considered as technical replicates. Mouse T cells were diluted to the final concentration 2×10^6 cells/mL in sterile cultural medium RPMI-1640 (Gibco, Paisley, Scotland, UK) containing 10% FBS and 0.1 M HEPES, pH 7.4. The resulting mouse T cell suspensions were used for all conditions and time points of experiment and non-treated control.

2.2. Cultured Human T Cells

An immortalized line of human T lymphocytes (human T cells) (Jurkat, Clone E6.1 TIB-152 (ATCC, Gaithersburg, MD, USA) was propagated from three frozen aliquots and subcultured cell stocks were used as sources for biological triplicates. Human T cells were diluted to final concentration 2×10^6 cells/mL in sterile cultural medium RPMI-1640 (Gibco, Paisley, Scotland, UK) containing 10% FBS and 0.1 M HEPES, pH7.4. The resulting human T cell suspensions were used for all conditions and time points of experiment and in non-treated control.

2.3. Experimental Platforms

The fast rotating clinostat (CL, DLR, Cologne, Germany), and random positioning machine (RPM, Dutch Space, Leiden, The Netherlands) were used in a comparative approach as ground-based facilities to simulate microgravity for suspension cell cultures of primary mouse T cells and cultured human T cells as described previously [16]. Applied regimes based on previous optimization experiments were as follows: 60 rpm for CL, continuously rotating around one rotation axis perpendicular to the direction of the gravity vector (Video S1), 12 rpm for RPM, consisting of 2 rotation axes, operated in the random direction mode (Video S2), and constantly 180 rpm for orbital hydrodynamic cell stress (HS)-inducing platform (Infors AG CH-4103 Minitron, Bottmingen, Switzerland) continuously rotating around one rotation axis parallel to the direction of the gravity vector. HS inducing platform was loaded with cylindrical external containers with a radius of 14 mm and HS sample tubes were placed into containers (Video S3). In the clinostat, cell suspension samples were exposed in 1 mL polystyrene pipettes with a radius of 1 mm. Thus, maximal residual acceleration of clinorotation did not exceed 0.04 g according to previously suggested formula and calculation [17,18]. In the RPM and HS platforms and in stationary 1 g non-treated control (NTC), cell samples were exposed in 5 mL polystyrene cylindrical tubes with a radius of 5 mm.

2.4. RNA Extraction

Total RNA was purified from sorted cells using RNeasy kit #74104 (QIAGEN, Hilden, Germany). Each RNA sample was treated with DNA nuclease using RNAse-free DNAse kit #79254 (QIAGEN, Hilden, Germany) during RNA isolation procedure to avoid contamination by genomic DNA. The concentration of purified total RNA was measured by NanoDrop 2000 (Thermo Scientific, Wilmington, DE, USA). RNA integrity and purity was visually evaluated by 1% UltraPureAgarose, #16500500 (Invitrogen, Waltham, MA, USA), 1xTAE gel electrophoresis analysis. Gel images were created with ImageQuant LAS 4000 LAS4000 Image system using ImageQuant LAS 4000 Control Software (GE Healthcare, Freiburg, Germany). To ensure the robustness of RNA sequencing and qPCR data, in each treatment group and in non-treated controls, only two samples with the best RNA quality and quantity values of three isolated RNA samples were selected and processed further to RNA-seq stage or to RT-qPCR (Table A7). All selected isolated RNA samples were subjected to and have passed both the internal quality control (QC) and the QC performed by sequencing company (Novogene, Hongkong).

2.5. Real-Time qPCR-Based Gene Expression Profiling

Two μg of total RNA per sample was used for each cDNA synthesis reaction (with SuperScript™ II Reverse Transcriptase, #18064-014 (Invitrogen). RT-qPCR reactions were performed using SsoAdvanced™ Universal SYBR® Green Supermix kit, #1725272SP with C1000/CFX96 RT-PCR System (Bio-Rad Laboratories, Hercules, CA, USA). Gene-specific primers were designed with PrimerBank software pga.mgh.harvard.edu/primerbank (accessed on 28 June 2018). (Supplementary Materials File S4). Gene expression profiling by real-time qPCR was performed, as described previously [19], in three technical replicates for each cDNA template sample, with Ct variation between triplicates less than cut-off +/− 0.25. Gene expression data: the mean of the technical triplicate, ΔCt, mean normalized RQ value of biological replicates and standard deviation between RQ of biological replicates were calculated and analyzed in Excel. All RT-qPCR data were normalized by values of cell culture non-treated control (NTC) included in cell culture experimental panels.

2.6. RNA-Seq and Bioinformatic Analysis

RNA sequencing and data quality control was performed with Illumina HiSeq-PE150 Platform at Novogene (Hongkong) (Table A5). Mapping to the reference genome was performed with HISAT2, v.2.0.5. Reads were aligned to the reference genome of the house mouse (Mus musculus) assembly December 2011 (GRCm38/mm10) (Table A6). Standard bioinformatics analysis of RNA-seq data was performed by Novogene (Hongkong), including primary data filtering to remove adaptor sequences, contamination, and low-quality reads from raw reads, reads alignment, genome-wide distribution of RNA-seq reads, gene ontology (GO) function analysis of corresponding genes and GO enrichment analysis [20]. RNA-seq differential gene expression analysis was performed with DESeq2 in R package. In gene expression analysis, H-cluster, K-means, and SOM were used to cluster the $\log_2$ (ratios) (Table A8) [21–23]. Functional classification of refined data for peak-related genes was performed using NCBI Gene resource www.ncbi.nlm.nih.gov (Bethesda, MD, USA) (accessed on 12 March 2021) and a gene list was generated in Excel (Baton Rouge, LA, USA).

3. Results

3.1. RNA-Seq

3.1.1. Transcript Distribution and Gene Expression Pattern

To setup the SMG experiment, cell suspensions of primary mouse thymocytes (mouse T cells) were subjected to HS inducing system or exposed to SMG in CL or RPM. After exposure to these conditions, the cells were processed for RNA isolation and generation of RNA library followed by RNA sequencing (RNA-seq). The differential gene expression analysis revealed arrays of genes differentially expressed in each of the experimental platforms—CL, RPM, and HS inducing system. Overall transcript expression levels showed a similar distribution range in different RNA-seq samples with high coincidence between biological replicates (Figure 2A). In hierarchical clustering of differentially expressed genes (DEGs), similar expression patterns were observed in samples after 8 h in SMG conditions, and it was possible to discern a distinct pattern of DEGs between SMG and HS-treated samples (Figure 2B). The set of transcripts shared between CL and RPM panels were considered to represent gene candidates of the specific mouse T cell transcriptome response to SMG (Figures 3 and 4).

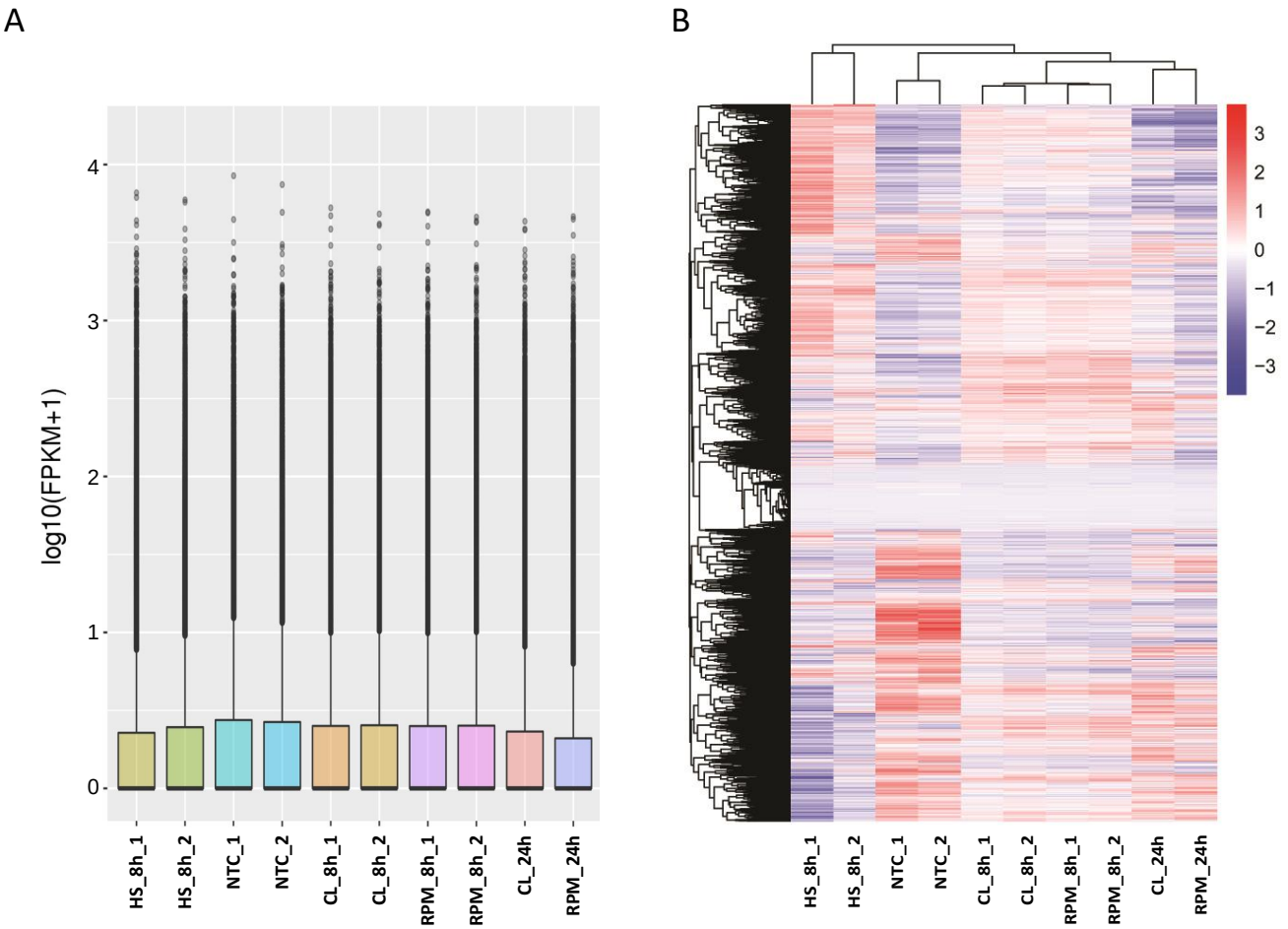

Figure 2. The overview of global transcriptome expression in RNA-seq samples (mouse T cells). (**A**) **FPKM distribution in RNA-seq samples**. Boxplot demonstrates the FPKM distribution in RNA-seq samples, the *x*-axis shows the sample names and the *y*-axis shows the $\log_{10}$(FPKM + 1) value. (**B**) **Heatmap of clustering of differential gene expression in RNA-seq samples.** The hierarchical cluster analysis was used to observe gene expression patterns under SMG or HS experimental conditions versus NTC. The color scale from red to blue represents the $\log_{10}$(FPKM + 1) value from high to low gene expression levels.

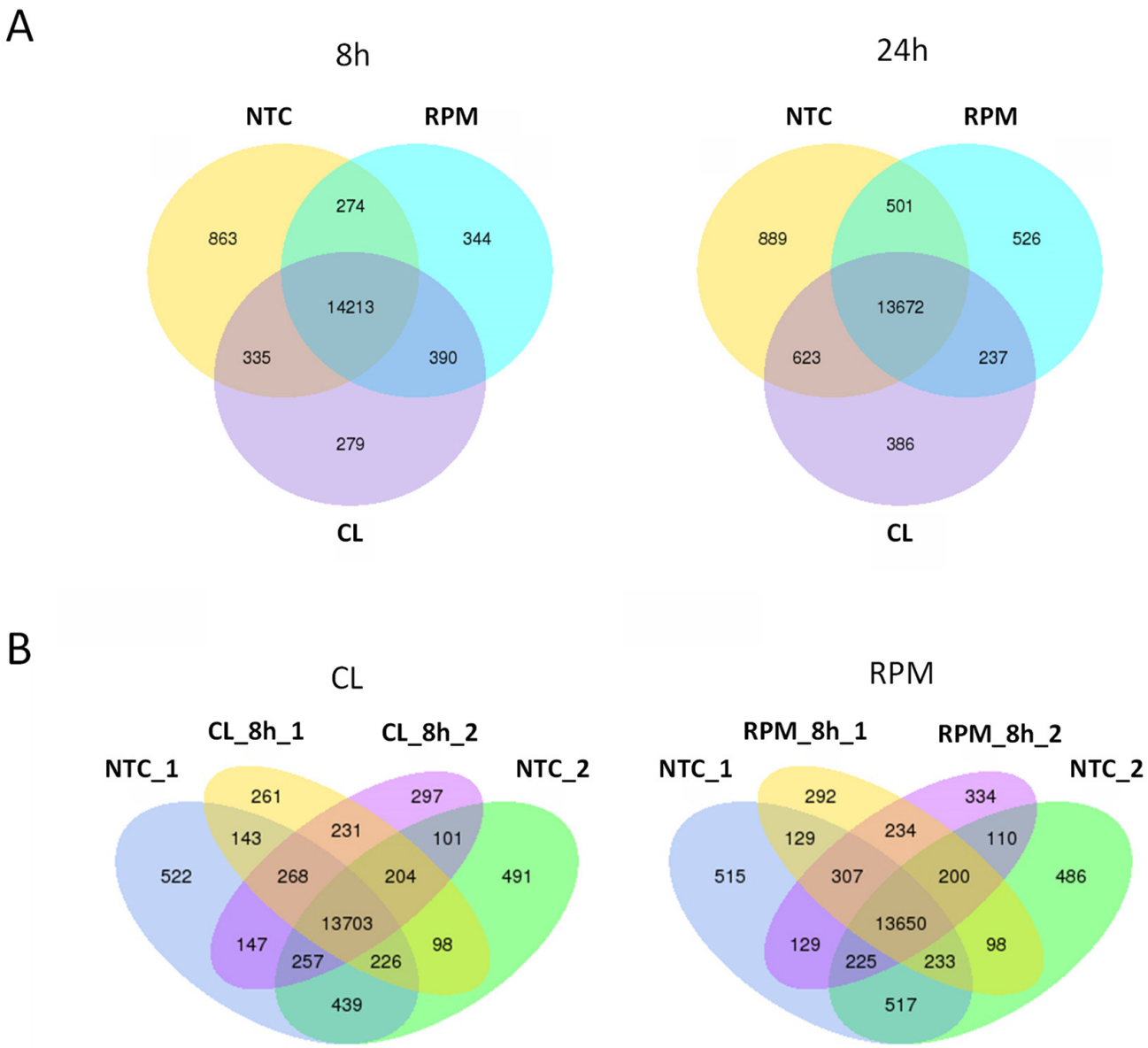

Figure 3. Venn diagrams indicating numbers of significantly expressed and co-expressed genes in mouse T cells in simulated microgravity experiment. (**A**) **Gene expression in simulated microgravity experiment at 8 h and 24 h**. Numbers of expressed and co-expressed genes shown at 8 h and 24 h of treatment by simulated microgravity in clinostat (CL) and random positioning machine (RPM) versus non-treated control (NTC). (**B**) **Gene expression in biological duplicates at 8 h of simulated microgravity**. Numbers of expressed and co-expressed genes indicated in biological duplicates at 8 h in clinostat (CL) experiment (CL_8h_1, CL_8h_2) and random positioning machine (RPM) experiment (RPM_8h_1, RPM_8h_2) versus biological duplicates of non-treated control (NTC_1, NTC_2).

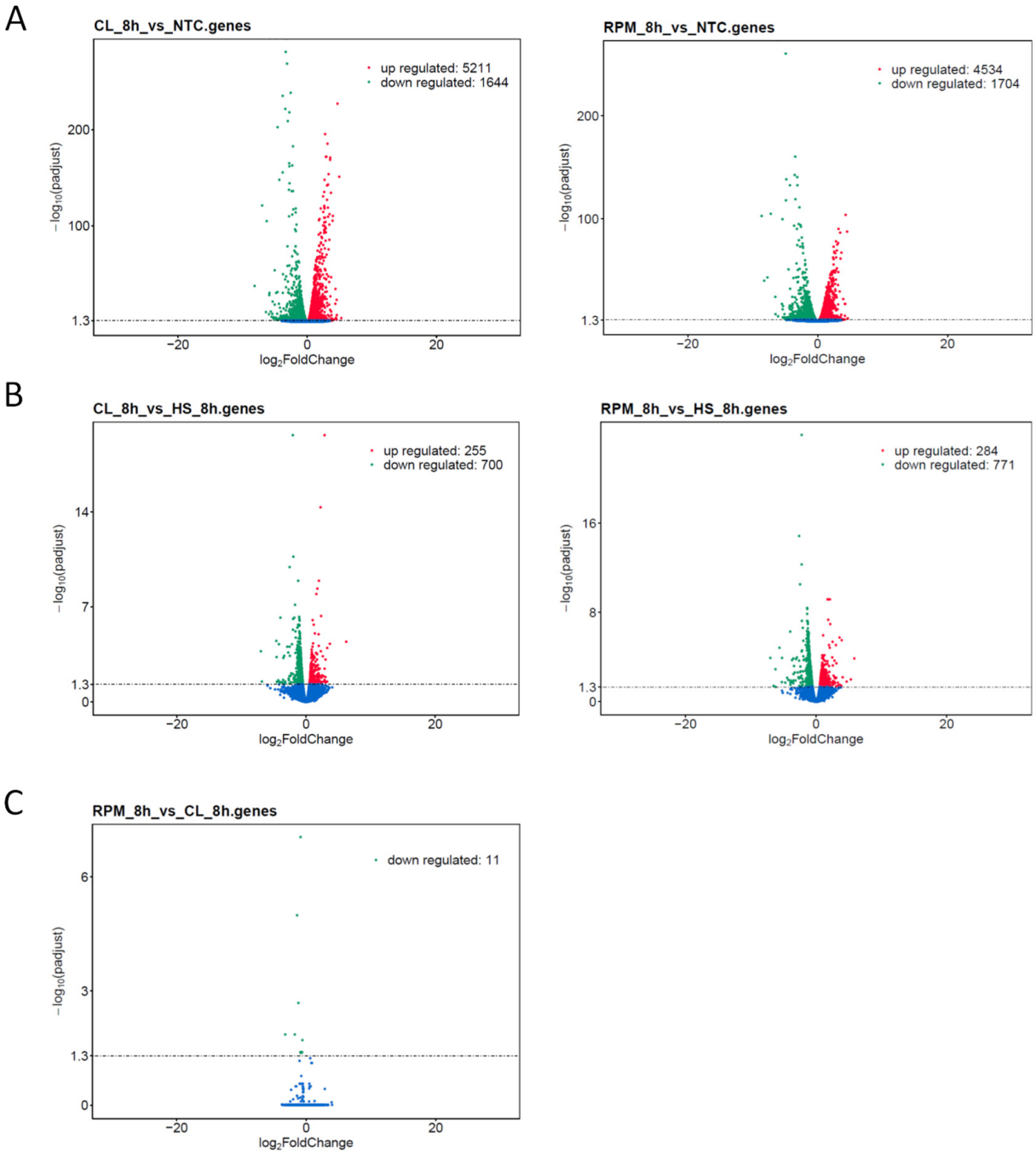

Figure 4. Volcano plots displaying overall distribution of differentially expressed genes in mouse T cells at 8 h of simulated microgravity. The *x*-axis shows the fold change in gene expression, and the *y*-axis designates the statistical significance of the differences between treatment group and control group with the threshold set as: padj < 0.05. Significantly up- and down-regulated genes highlighted in red and green, respectively, and other genes shown in blue. Treatment group versus control group data illustrated for comparisons: (**A**) **Treatment by simulated microgravity in clinostat (CL) and random positioning machine (RPM) versus non-treated control (NTC).** (**B**) **Treatment by simulated microgravity in clinostat (CL) and random positioning machine (RPM) versus hydrodynamic stress (HS).** (**C**) **Treatment by simulated microgravity in random positioning machine (RPM) versus clinostat**.

3.1.2. Gene Ontology

The number of terms in the Gene Ontology (GO) function analysis of corresponding genes and GO enrichment analysis was considerably lower when comparing SMG to HS treatment in contrast to the comparison of SMG to non-treated control (NTC) samples. This was true for all three categories of GO enrichment analysis: cellular component (CC), molecular function (MF), and biological processes (BP) (Figure A2). For transcription regulation, counts of MF term, "transcription factor binding, GO:0008134", were 271 in CL vs. NTC; 226 in RPM vs. NTC and 35 in CL vs. HS; 33 in RPM vs. HS, respectively. Counts of MF term "DNA-binding transcription factor activity, GO:0003700" were 279 in CL vs. NTC; 247 in RPM vs. NTC and 26 in CL vs. HS; 30 in RPM vs. HS, respectively. For organization of cytoskeleton, counts of the CC term, "cytoskeleton, GO:0005856", were 904 in CL vs. NTC; 782 in RPM vs. NTC and 132 in CL vs. HS; 161 in RPM vs. HS, respectively. Counts of the BP term, "cytoskeleton organization, GO:0007010", were 492 in CL vs. NTC; 429 in RPM vs. NTC and 74 in CL vs. HS; 95 in RPM vs. HS, respectively. Counts of MF term, "cytoskeletal protein binding, GO:0008092", were 319 in CL vs. NTC; 280 in RPM vs. NTC and 49 in CL vs. HS; 68 in RPM vs. HS, respectively (Figure A2; Supplementary Materials File S1). The top five common terms for RPM vs. HS and CL vs. HS at 8 h of simulated microgravity are shown for three categories of GO enrichment analysis: CC, MF, and BP (Table A1).

3.1.3. Co-Expression DEG Analysis

In co-expression analysis, the number of significantly co-expressed genes detected in common between the two biological replicates in the CL and RPM experiments at 8 h of SMG were quite similar: 231 and 234 genes, respectively (Figure 3). To identify genes that were co-expressed in both CL and RPM platforms at 8 h of simulated MG, the lists of 231 genes and 234 genes were compared and 113 common genes were identified (Supplementary Materials File S2). Out of these 113 genes, 65 genes were known to be expressed in thymocytes (18 high or moderately expressed genes and 47 low expressed genes), and the remaining 48 genes were represented by pseudogenes, ncRNAs, and unknown sequences. Above, 65 genes were estimated for the significance of the transcript expression at 8 h in simulated MG versus HS (Supplementary Materials File S3), which resulted in the list of seven genes found to be significantly differentially expressed, of which five were protein-coding genes expressed in murine thymocytes (Table A2).

Fam163b with unknown function was the only significantly down-regulated gene in both CL and RPM samples vs. HS condition. DEGs down-regulated at 8 h in RPM vs. HS included 2′-deoxynucleoside 5′-phosphate N-hydrolase 1 (*Dnph1*), also known as *RCL*; *C6orf108*; *dJ330M21.3*, a putative oncogene with a role in cellular proliferation and c-Myc-mediated transformation [24]. Interestingly, *DNPH1* was shown to be down-regulated post-flight in the NASA twins study [25]. Another gene in this group was X-linked Kx blood group related 5 (*Xkr5*), also known as *XRG5*; *5430438H03Rik* gene, involved in the engulfment of apoptotic cell corpses [26]. Two other significantly expressed DEGs, tripartite motif-containing 34 (*Trim34*) and uroplakin-1b (*Upk-1b*), were found to be up-regulated and down-regulated at 8 h in CL vs. HS, respectively. The human homolog TRIM34, was shown to facilitate the formation of multinucleated giant cells by enhancing cell fusion [27]. Uroplakin-1b, also known as Tsp, belong to the tetraspanin family. Most tetraspanins are cell-surface proteins that mediate signal transduction in the regulation of cell development, activation, growth, cell migration, and motility [28,29].

As was the case with the GO enrichment analysis, the number of genes in the DEG analysis was considerably lower when comparing SMG treatment and HS control samples versus comparing SMG treatment and non-treated controls (NTC). The number of up-regulated/down-regulated transcripts were 255 and 700 in CL versus HS; 284 and 771 in RPM versus HS; 5211 and 1644 in CL versus NTC; 4534 and 1704 in RPM versus NTC, respectively (Figure 4A,B).

In addition, DEG analysis revealed 11 transcripts that were found specifically induced in the CL system versus RPM platform (Figure 4C, Table A3). Several of these genes are conserved in higher Vertebrata and expressed in mouse and human T cells and are of particular interest: *Hspa1a*, *Cd74*, *Fscn1*, *Rnaset2b*, *Pif1*. Ubiquitously expressed chaperone heat shock protein 1A (also known as Hspa1a, Hsp70) stabilizes proteins against aggregation and mediates protein folding [30]. The CD74 antigen (CLIP, DHLAG, etc.) also serves as an important chaperone in immune cells and plays a role in initiation of survival pathways and cell proliferation [31]. Fascin actin-bundling protein 1 (fascin-1, Fscn1, Fan1) is involved in actin cytoskeleton organization and biogenesis and acts within actin filament bundle assembly. The encoded protein plays a critical role in cell migration, motility and cell adhesion [32,33]. Ribonuclease T2 (Rnaset2b) regulates mitochondrion-associated cytosolic ribosomes [34]. PIF1 5′-to-3′ DNA helicase (Pif1) resolves G-quadruplexes and RNA-DNA hybrids at the ends of chromosomes and also prevents telomere elongation by inhibiting the actions of telomerase [35,36]. These and a few other genes represent a unique gene signature which discriminates SMG treatments in RPM and CL.

3.2. Real-Time qPCR DEG Analysis

The gene expression of selected 27 genes related to or involved in the actin cytoskeleton networks was compared in cultured human T cells (Jurkat) under simulated MG in both CL and RPM using RT-qPCR. The DEGs profiles showed similar patterns for most of the considered genes in both CL and RPM simulators (Figure 5A). Gene expression changes were compared between cells that were subjected to simulated MG and HS. The 27 genes were grouped into those in which the expression was greater, less than, and equal to the expression in simulated MG when compared to the expression in HS. From this comparison of DEGs, it was possible to identify genes in which the change in expression was specific to either simulated MG or to HS (Figures 5B and A3, Table A4). The members of the VAV family of guanine nucleotide exchange factors VAV1-3 were down-regulated in SMG, while their expression was constant in HS. The VAV proteins mediate changes in the actin cytoskeleton via control of the small Rho GTPases [37,38]. The expression of the *NFATC2* gene encoding a transcription factor important for the development and differentiation of T cells [39] was suppressed in SMG while unchanged in HS (Figure 5B). Candidate marker genes of the T cell response to HS were identified. Among these were genes encoding integrins that play a key role in intracellular adhesion and cell–cell interactions and members of the Rac family of small GTPases mediating changes in the actin cytoskeleton, for example, in cell adhesion and lamellipodium formation [40]. The expression of *ITGAL*, *ITGB1*, *ITGB2*, *RAC1*, and *RAC2* was reduced in the cells under HS but not in cells in simulated MG. Therefore, differential gene expression changes specific to both the response to SMG and HS were identified (Figures 5C and A3).

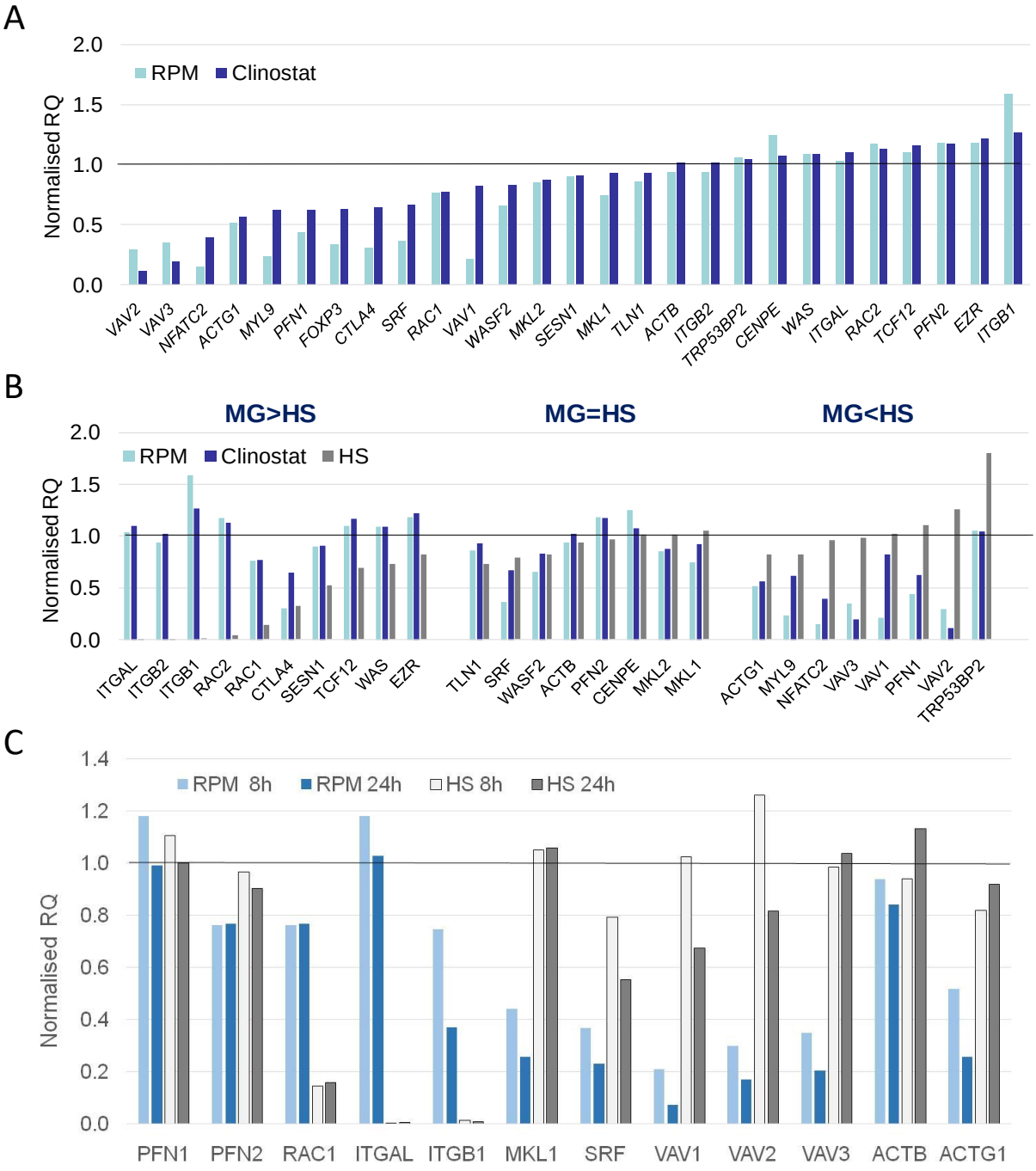

Figure 5. Differentially expressed genes in human T cells (Jurkat) in simulated microgravity experiment measured by RT-qPCR. (**A**) **Actin cytoskeleton network differential gene expression response to simulated microgravity**. Differential expression of 27 genes measured at 8 h of simulated microgravity in random positioning machine (RPM) or clinostat and normalized by values of non-treated control (RQ value equals 1.0). (**B**) **Candidate marker genes discriminating T cell responses to simulated microgravity and to hydrodynamic stress**. Differential expression measured at 8 h of treatment in random positioning machine (RPM), clinostat, or hydrodynamic cell stress-inducing platform (HS). Genes grouped according to T cell responses in MG and HS for gene expression higher in simulated microgravity (MG > HS) or in hydrodynamic stress treatment (MG < HS) or in a similar range (MG = HS). (**C**) **Dynamic expression of actin network selected key genes in simulated microgravity versus hydrodynamic stress response**. Differential expression measured at 8 h and 24 h of treatment in random positioning machine (RPM) or hydrodynamic stress-inducing platform (HS) and normalized by non-treated control (NTC) values (RQ value equals 1.0).

Gene expression changes in Jurkat cells were also analyzed at both 8 and 24 h. This provided a dynamic view of gene expression and the trends in expression over time could be identified. The expression level of *PFN1* and *RAC1* was relatively constant in CL and RPM at both time points. However, *RAC1* was further down-regulated in response to HS when compared to simulated MG. *PFN1* encodes profilin 1, a regulator of actin filament formation [41]. The integrin genes *ITGAL* and *ITGB1* showed the same trend in gene expression and were down-regulated in response to HS. Under simulated MG, their expression decreased over time from 8 h to 24 h. *MKL1/MRTFA* expression was constant in response to HS but decreased in simulated MG and was further reduced over time from 8 h to 24 h. *MKL1/MRTFA* encodes an actin sensor that upon decreased G-actin enters into the nucleus and interacts with the serum response factor (SRF) to drive transcription of actin network genes [13,14]. *VAV1*, *VAV2*, and *VAV3* all followed the same trend in gene expression. There was a greater reduction in expression in response to SMG conditions while a decrease in expression was seen at 24 h in both SMG and HS. All of these genes are involved in or closely related to regulation of the actin cytoskeleton. The expression of genes encoding actin β and actin γ1 was analyzed and compared at both 8 and 24 h. This revealed an opposing trend in response to HS and simulated MG at the level of actin expression. Cells exposed to SMG had down-regulated *ACTB* and *ACTG1*, and the trend in time was a further reduction in expression. In contrast, there was an increase in the expression of *ACTB* and *ACTG1* relative to the NTC, which further increased between 8 and 24 h.

Together, SMG and HS both have an influence on the actin cytoskeleton network of T cells at the level of gene expression. However, the response is in opposing directions with an increase in actin expressionin cells under HS, while actin expression levels decreased in SMG.

4. Discussion

T cells constitute an important part of immune system that is affected by microgravity conditions and becomes compromised during or following the space flights in a large cohort of astronauts [7,9,11,42].

Although not replacing the possibilities of expensive and rare experiments on the effects of weightlessness at Earth orbital facilities, the SMG platforms proved to be valuable tools to study the nature of cellular mechanisms and gravisensing processes in ground-based wet laboratory settings [16]. In this project, the T cell response to SMG conditions was studied at the level of gene expression in primary mouse T lymphocytes (thymocytes) and cultured human T lymphocytes (Jurkat) using two ground-based applied systems: fast rotating clinostat (CL) and random positioning machine (RPM) (Figure A1). Treatment was performed for 8–24 h in sealed plastic tubes at 37 °C in complete RPMI-1640 cell culture medium. In CL, the position of the sample is constantly changed around one axis with respect to the direction of Earth's gravity vector and MG is simulated when the position of the sample changes faster than the sample can respond to gravity [43]. RPM uses the same underlying principle to simulate MG, however, rotation is performed around two axes in random mode (Figure 1A) [44]. In biological, in vitro experiments, non-treated control (NTC) traditionally is used as a best guess normalizer in the data analysis. However, both selected rotational SMG platforms employ forced cell movement in liquid. Therefore, an important consideration when using these MG simulators is that cell samples are rotating in a viscous cultural media exposing cells to shear forces which induces hydrodynamic stress (HS). Commonly, HS was also found in microchannels of microfluidic and flow cytometry systems, in bioreactors where it has been shown to induce apoptosis and cause changes in the cytoskeleton of cells [45–48], and in the cells of tissues exposed to mechanical forces of physiological fluids [49–51]. Methodically, it is crucial to be able to distinguish cell responses to the studied factor (treatment) and to other factors present in the experimental system. By that reasoning,

the inclusion in our study of additional rotational HS-only inducing platform as a dynamic control was essential.

Therefore, in order to distinguish between gene expression changes induced by MG from those caused by response to HS, T cells in MG simulators were compared to those subjected to HS alone in the same type of plastic tubes and culture medium at the same temperature in a rotating orbital shaker for 8–24 h (Figure 1B). Inclusion of NTC and HS samples in the study as the parallel controls showed that the use of HS for data normalization decreased the transcriptome expression value noise considerably (Figure 4A,B) and highlighted gene ontology (GO) terms that are specific for T cell transcriptome response to SMG (Figure A2). Since T cell cytoskeleton is involved in many functions of lymphocytes, such as cell migration and cell-cell interactions, it is possible that the impact of microgravity on the cytoskeleton causes the immunosuppression experienced by the astronauts. Analysis of gene expression response at different time points demonstrates certain dynamics of T cell response to SMG. Moreover, a number of genes encoding constituents of actin cytoskeleton network genes changes expression in SMG with time that was confirmed by RT-qPCR (Figure 5C). Notably, T cell transcriptome responses to 8 h of SMG treatment in clinostat (CL) and random positioning machine (RPM) appeared to cluster together and have quite similar gene expression patterns (Figures 2B and 5A). However, a closer look at these responses and the comparison of differential expression at this timepoint revealed a panel of 10 genes known to be expressed in thymocytes. As these 10 genes were found to be up-regulated in clinostat platform treatment versus RPM system (Figure 4C, Table A3), one may speculate that their expression is inhibited, probably due to higher shear stress that was previously observed in RPM when compared to clinostat conditions [52].

To conclude, five genes (*Fam163b*, *Dnph1*, *Xkr5*, *Trim34*, *Upk-1b*) found to be differentially expressed in murine T cells in SMG platforms vs. HS platform (see Section 3.1.3. Co-expression DEG analysis, Table A2), represent new candidate gene targets to investigate further the cell response to microgravity. On the other hand, a panel of 10 DEGs (Table A3) up-regulated in clinostat vs. RPM comparison speaks for sensitivity of effects observed in SMG platforms to shear forces due to imposed cell movement in culture medium. Gene expression patterns obtained in the current work could be different in space, and hence need to be validated in orbital studies and/or in stressless ground systems. Finally, a fresh look from a new perspective at transcriptomics study practice allowed to distinguish two types of cell response and will help to distill the actual reactions of biological systems to weightlessness in future ground-based and orbital translational research.

Funding: This work was supported by research grant SNSB 2018-R from the Swedish National Space Agency.

Supplementary Materials: The following supporting information can be downloaded at: https://www.mdpi.com/article/10.3390/ijtm2030029/s1; Files S1–S4 (Excel), Videos S1–S3 (MP4): File S1—List of Gene Ontology (GO) terms, File S2—Venn diagram genes, File S3—Genes expressed in thymocytes, File S4—Primers used in RT-qPCR, Video S1—Clinostat (CL), Video S2—Random positioning machine (RPM), Video S3—Hydrodynamic stress inducing platform (HS).

Informed Consent Statement: All animal experiments performed are approved by the Stockholm North Animal Ethics Committee permits N272/14 and 11159-18.

Data Availability Statement: The datasets presented in this study can be found in online repositories. The name of the repository and accession number can be found below: National Center for Biotechnology Information (NCBI) Gene Expression Omnibus (GEO), www.ncbi.nlm.nih.gov/geo/, GSE200513 (accessed on 24 March 2022).

Acknowledgments: The author thanks colleagues at the Institute of Aerospace Medicine at the German Aerospace Center in Cologne, Germany, Karolinska Institutet in Stockholm, Sweden for providing access to lab facilities and Amgen Scholar Program participants for assistance and comments on the manuscript.

Conflicts of Interest: The author declares no conflict of interest.

Appendix A

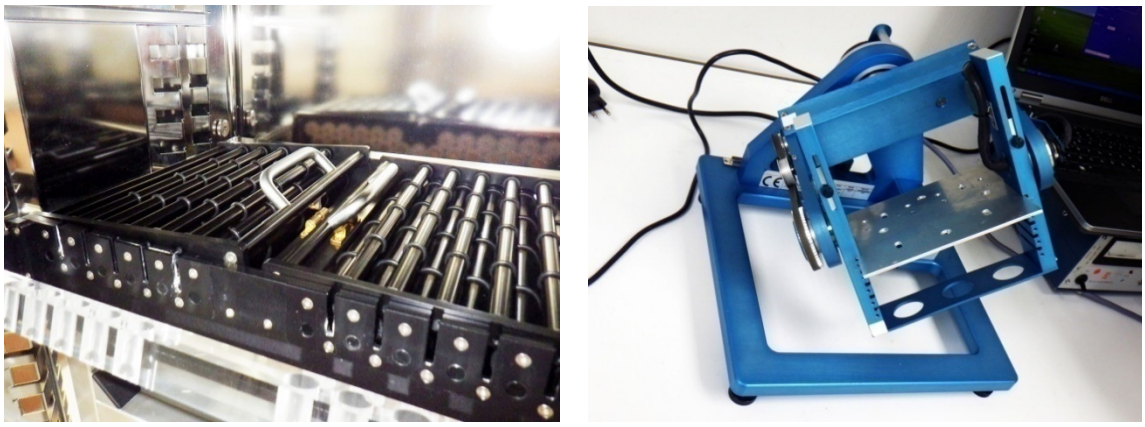

(**A**) (**B**)

Figure A1. Simulated microgravity platforms: Microgravity simulation platforms (DLR) used as key experimental systems to simulate microgravity for suspension cell cultures: (**A**) Clinostat, (**B**) Random positioning machine.

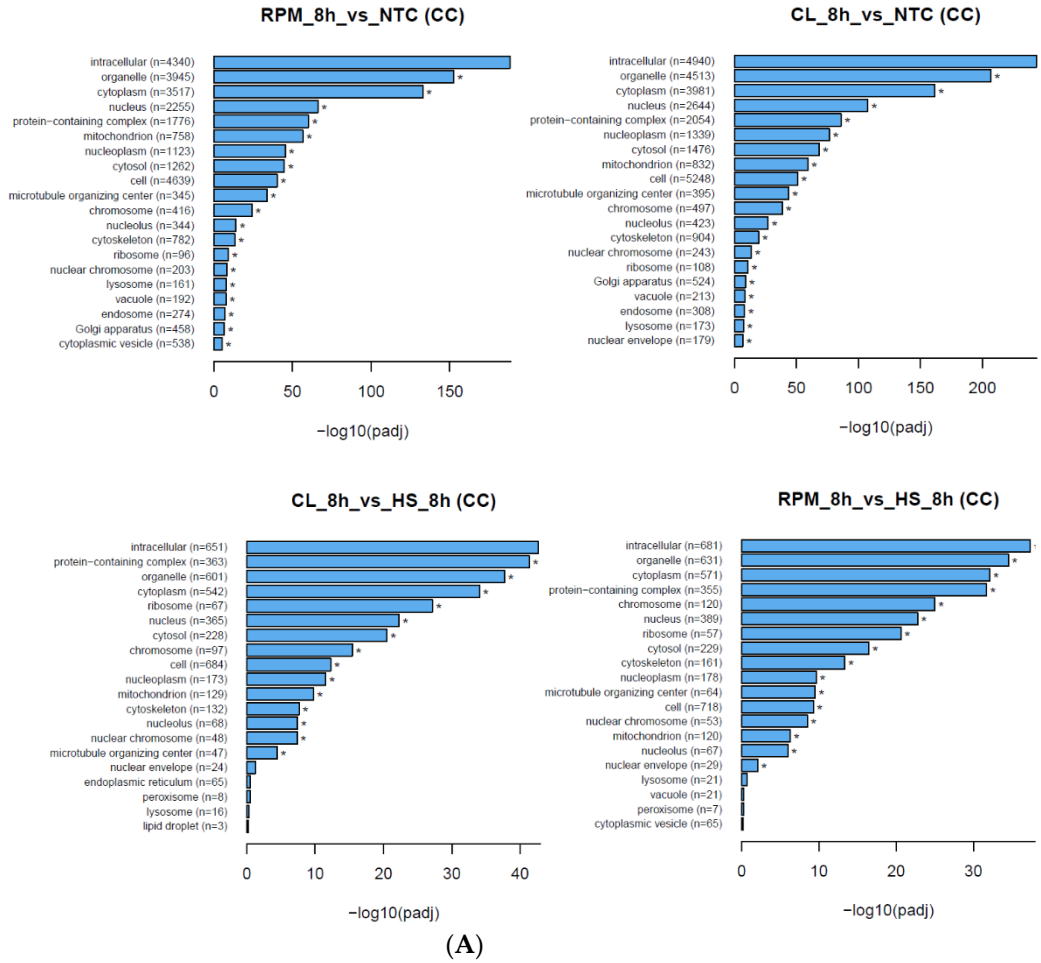

(**A**)

Figure A2. *Cont.*

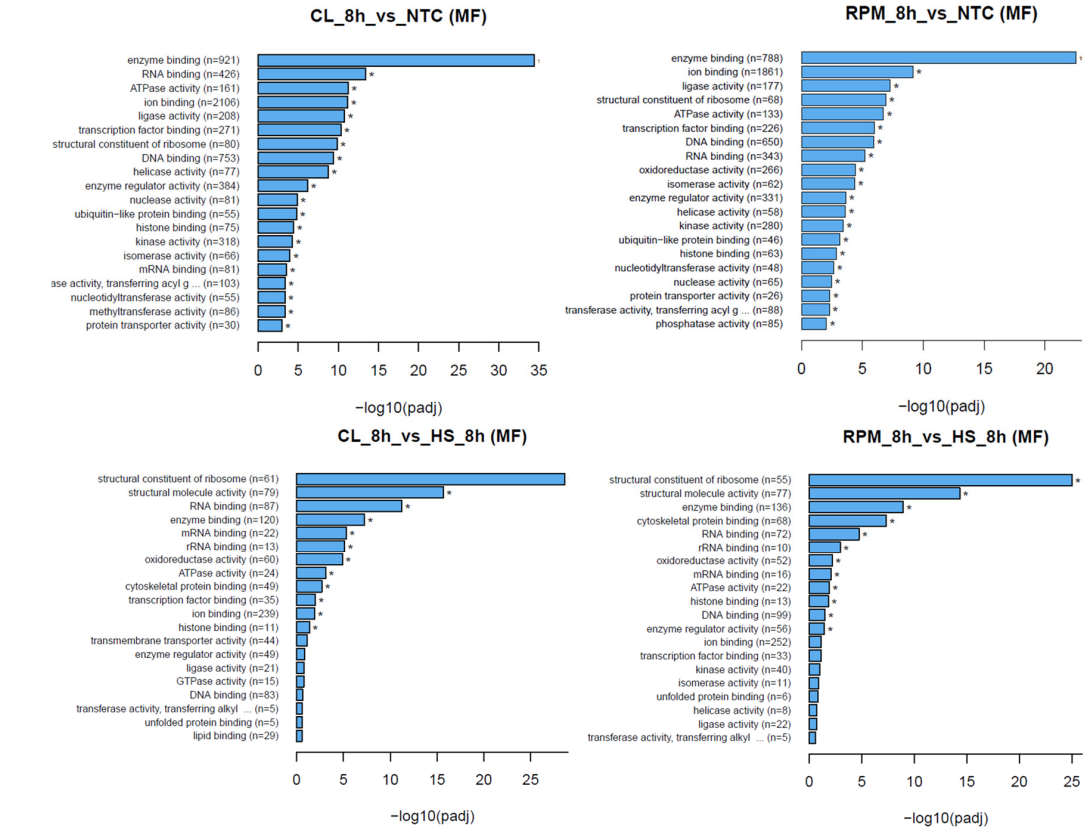

(**B**)

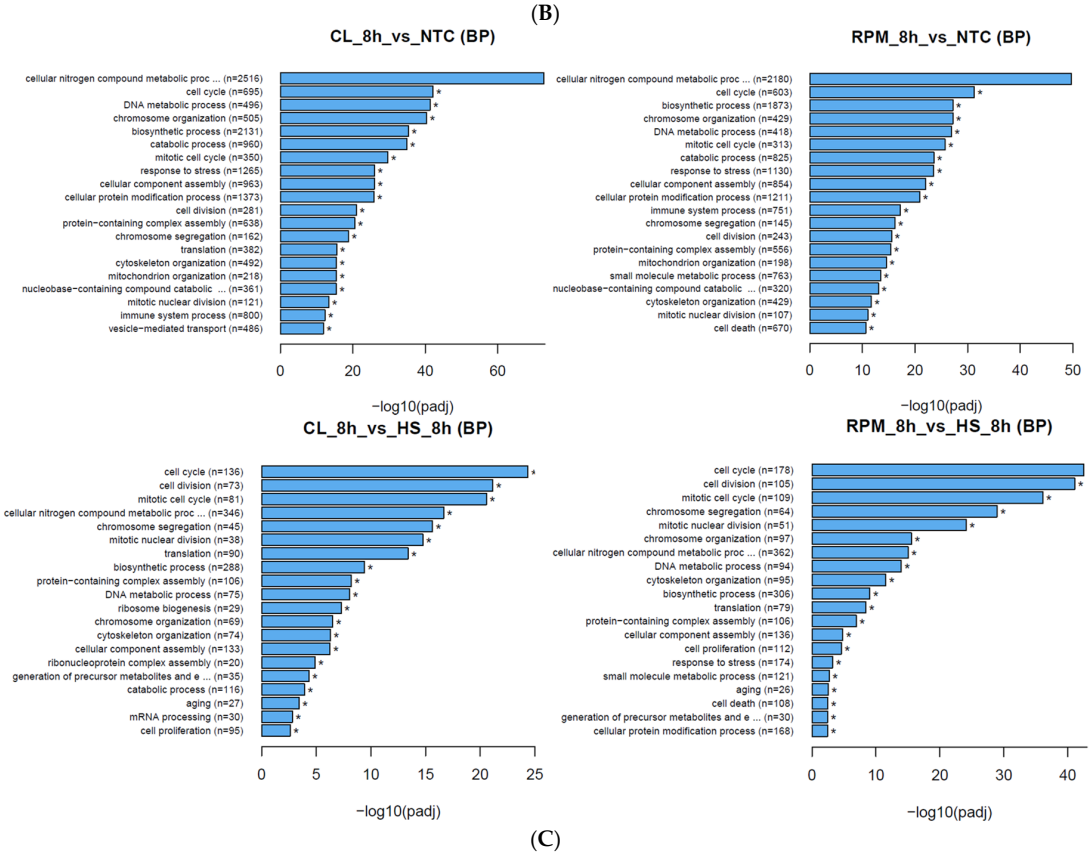

(**C**)

Figure A2. Gene Ontology (GO) enrichment analysis. Treatment versus control comparison for: (**A**) Cellular component (CC), (**B**) molecular function (MF), and (**C**) biological processes (BP) terms. * denotes significantly enriched GO terms. Top 20 significantly enriched GO terms are shown.

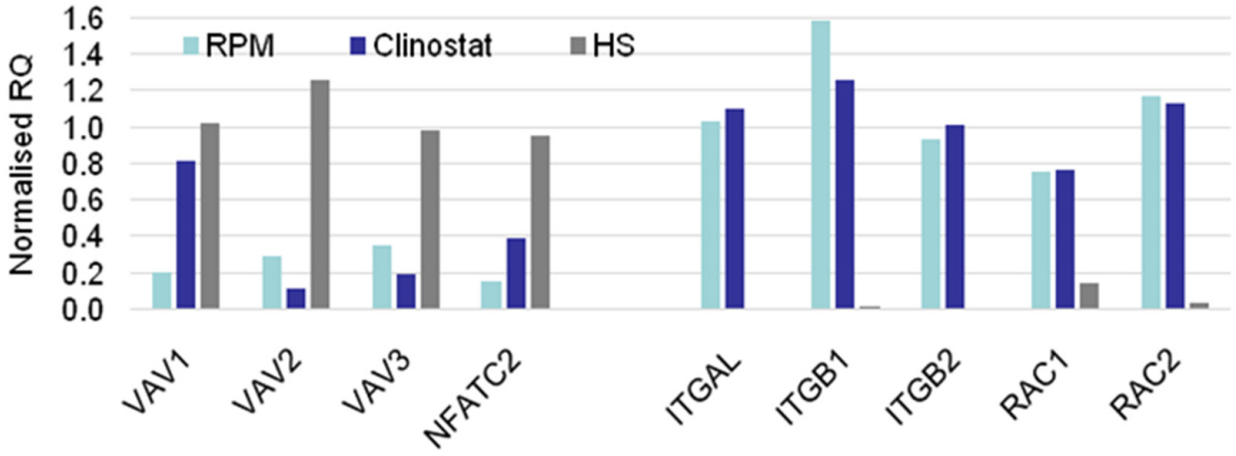

Figure A3. Candidate marker genes discriminating T cell transcriptome responses: Selected differentially expressed genes of actin cytoskeleton network and related genes can be used as potential markers for the response of T cells to simulated microgravity (MG) platforms (clinostat and random positioning machine (RPM)), and to hydrodynamic stress (HS).

Appendix B

Table A1. Top five common Gene Ontology (GO) terms at 8 h of simulated microgravity in RPM and CL versus hydrodynamic stress (HS) treatment for three categories of GO enrichment analysis: cellular component (CC), molecular function (MF), and biological processes (BP).

GO Category	GO Term ID	Description	Count, RPM vs. HS, 8 h	Count, CL vs. HS, 8 h	*p*-Value, RPM vs. HS, 8 h	*p*-Value, CL vs. HS, 8 h
CC	0043226	organelle	631	601	1.0982×10^{-36}	4.1886×10^{-40}
CC	0005737	cytoplasm	571	542	3.4794×10^{-34}	2.6777×10^{-36}
CC	0005634	nucleus	389	365	1.5571×10^{-24}	3.0424×10^{-24}
CC	0032991	protein-containing complex	355	363	1.001×10^{-33}	6.768×10^{-44}
CC	0005694	chromosome	120	97	7.3686×10^{-27}	4.2603×10^{-17}
MF	0019899	enzyme binding	136	120	2.0757×10^{-10}	0019899
MF	0005198	structural molecule activity	77	79	5.9878×10^{-16}	2.0991×10^{-17}
MF	0003723	RNA binding	72	87	4.4686×10^{-06}	0003723
MF	0008092	cytoskeletal protein binding	68	49	9.5479×10^{-09}	0008092
MF	0003735	structural constituent of ribosome	55	61	6.5833×10^{-27}	8.7689×10^{-31}
BP	0034641	nitrogen compound metabolic process	362	346	1.1454×10^{-16}	2.0049×10^{-18}

Table A1. *Cont.*

GO Category	GO Term ID	Description	Count, RPM vs. HS, 8 h	Count, CL vs. HS, 8 h	*p*-Value, RPM vs. HS, 8 h	*p*-Value, CL vs. HS, 8 h
BP	0009058	biosynthetic process	306	288	1.6028×10^{-10}	6.6327×10^{-11}
BP	0007049	cell cycle	178	136	2.4143×10^{-45}	2.2782×10^{-26}
BP	0006950	response to stress	174	152	0.00015733	0.0079929
BP	0022607	cellular component assembly	136	133	3.6597×10^{-6}	1.3117×10^{-7}

Table A2. The significantly differentially expressed genes in CL or RPM or both platforms at 8 h of simulated microgravity versus hydrodynamic stress treatment.

Gene ID	Gene Symbol	GENE NAME	T Cell Gene Expression	Log2 Fold Change CL vs. HS, 8 h	Log2 Fold Change RPM vs. HS, 8 h
109349	*Fam163b*	family with sequence similarity 163, member B	+	−1.06	−1.24
381101	*Dnph1*	2′-deoxynucleoside 5′-phosphate N-hydrolase 1	+	ns *	−1.44
434218	*Trim34b*	tripartite motif-containing 34B	+	2.83	ns
319581	*Xkr5*	X-linked Kx blood group related 5	+	ns	−1.40
	Upk1b	uroplakin−1b	+	−1.69	ns
6608222	*LOC6608222*	sodium/calcium exchanger protein	-	ns	−1.28
-	*Gm26737*	lncRNA, predicted gene, 26737	-	ns	−1.55

* ns—no significance.

Table A3. The significantly down-regulated genes in CL platform versus RPM platform at 8 h of simulated microgravity treatment.

Gene ID	Gene Symbol	Gene Name	T Cell Gene Expression	Log2 Fold Change RPM vs. CL, 8 h	Log2 Fold Change CL/RPM vs. HS, 8 h
68195	*Rnaset2b*	ribonuclease T2B	+	−0.87	ns/ns *
16149	*Cd74*	CD74 antigen	+	−0.69	ns/−1.2
14086	*Fscn1*	fascin actin-bundling protein1	+	−1.21	0.82/ns
208084	*Pif1*	PIF1 5′-to-3′ DNA helicase	+	−0.61	ns/−0.83
108956	*Apol7c*	apolipoprotein L 7c	+	−1.69	2.86/1.46

Table A3. *Cont.*

Gene ID	Gene Symbol	Gene Name	T Cell Gene Expression	Log2 Fold Change RPM vs. CL, 8 h	Log2 Fold Change CL/RPM vs. HS, 8 h
100042807	*Eif3j2*	eukaryotic translation initiation factor 3 s.J2	+	−1.75	ns/ns
193740	*Hspa1a*	heat shock protein 1A	+	−3.24	ns/ns
12316	*Aspm*	abnormal spindle microtubule assembly	+	−0.57	ns/ns
17476	*Mpeg1*	macrophage expressed gene 1	+	−0.90	ns/ns
14969	*H2-Eb1*	histocompatibility 2, class II antigen E beta	+	−0.80	ns/−1.23
432447	*Gm9824*	predicted pseudogene 9824	−	−0.81	ns/−0.99

* ns—no significance.

Table A4. Three groups of actin cytoskeleton network and related genes according to their relative differential gene expression levels in response of human T cells to simulated microgravity (MG) and under hydrodynamic stress (HS) confirmed by using RT-qPCR.

Relative Gene Expression.		
MG > HS	**MG = HS**	**MG < HS**
CTLA4	*ACTB*	*ACTG1*
EZR	*CENPE*	*FOXP3*
ITGAL	*MKL1*	*MYL9*
ITGB1	*MKL2*	*NFATC2*
ITGB2	*PFN2*	*PFN1*
RAC1	*SRF*	*TRP53BP2*
RC2	*TLN1*	*VAV1*
SESN1	*WASF2*	*VAV2*
TCF12		*VAV3*
WAS		

Table A5. RNA-seq data Quality Control summary.

Sample Name	Raw Reads	Clean Reads	Raw_Data (G)	Clean_Data (G)	Error_Rate (%)	Q20 (%)	Q30 (%)	GC_Content (%)
HS_8h_1	22275588	21763739	6.7	6.5	0.02	98.35	94.96	44.63
HS_8h_2	25204052	24721513	7.6	7.4	0.02	98.22	94.63	49.22
NTC_1	21231374	21054307	6.4	6.3	0.03	97.79	93.58	48.93
NTC_2	20185658	20021323	6.1	6.0	0.02	98.21	94.53	49.63
CL_8h_1	24315174	23786569	7.3	7.1	0.02	98.22	94.66	49.26
CL_8h_2	23844401	23296130	7.2	7.0	0.02	98.19	94.57	49.18
RPM8h_1	25600529	25051563	7.7	7.5	0.02	98.20	94.61	50.06
RPM8h_2	22988902	22513805	6.9	6.8	0.02	98.07	94.39	48.78
CL_24h	27021052	26760888	8.1	8.0	0.03	97.63	93.13	48.71
RPM24h	21106398	20567883	6.3	6.2	0.02	98.22	94.61	49.56

Table A6. Overview of RNA-seq data Mapping Status.

Sample Name	Total Reads	Total Mapped	Multiple Mapped	Uniquely Mapped	Read 1	Read 2	Reads Map to '+'	Reads Map to '−'
HS_8h_1	43527478	41999085 (96.49%)	1920836 (4.41%)	40078249 (92.08%)	20065964 (46.10%)	20012285 (45.98%)	20033591 (46.03%)	20044658 (46.05%)
HS_8h_2	49443026	47804795 (96.69%)	1935536 (3.91%)	45869259 (92.77%)	22985377 (46.49%)	22883882 (46.28%)	22924203 (46.36%)	22945056 (46.41%)
NTC_1	42108614	40639633 (96.51%)	1341423 (3.19%)	39298210 (93.33%)	19725847 (46.85%)	19572363 (46.48%)	19643692 (46.65%)	19654518 (46.68%)
NTC_2	40042646	38799106 (96.89%)	1315043 (3.28%)	37484063 (93.61%)	18781111 (46.90%)	18702952 (46.71%)	18737591 (46.79%)	18746472 (46.82%)
CL_8h_1	47573138	46039566 (96.78%)	1665988 (3.50%)	44373578 (93.27%)	22228572 (46.73%)	22145006 (46.55%)	22179441 (46.62%)	22194137 (46.65%)
CL_8h_2	46592260	45158442 (96.92%)	1615703 (3.47%)	43542739 (93.45%)	21819540 (46.83%)	21723199 (46.62%)	21763512 (46.71%)	21779227 (46.74%)
RPM8h_1	50103126	48551851 (96.90%)	1743876 (3.48%)	46807975 (93.42%)	23452298 (46.81%)	23355677 (46.62%)	23394967 (46.69%)	23413008 (46.73%)
RPM8h_2	45027610	43384044 (96.35%)	1601933 (3.56%)	41782111 (92.79%)	20937166 (46.50%)	20844945 (46.29%)	20883276 (46.38%)	20898835 (46.41%)
CL_24h	53521776	50474422 (94.31%)	1761017 (3.29%)	48713405 (91.02%)	24427089 (45.64%)	24286316 (45.38%)	24348363 (45.49%)	24365042 (45.52%)
RPM24h	41135766	39828513 (96.82%)	1328387 (3.23%)	38500126 (93.59%)	19287634 (46.89%)	19212492 (46.71%)	19243508 (46.78%)	19256618 (46.81%)

Table A7. Cell samples used in simulated microgravity (SMG) and hydrodynamic stress (HS) experiments or in non-treated controls (NTC).

Sample ID #	Sample Group	Biological Replicate ID	Biological Source	Treatment	Time Point	Downstream Application
T1	**HS_8h**	HS_8h_1	Primary T cells, *Mus musculus*	HS	8 h	RNA-seq
T2		HS_8h_2				RNA-seq
T3		HS_8h_3				-
T4	**NTC_8h**	NTC_8h	Primary T cells, *Mus musculus*	NTC	8 h	RNA-seq
T5		NTC_8h				RNA-seq
T6		NTC_8h				-
T7	**CL_8h**	CL_8h_1	Primary T cells, *Mus musculus*	CL	8 h	RNA-seq
T8		CL_8h_2				RNA-seq
T9		CL_8h_3				-
T10	**RPM_8h**	RPM_8h_1	Primary T cells, *Mus musculus*	RPM	8 h	RNA-seq
T11		RPM_8h_2				RNA-seq
T12		RPM_8h_3				-
T13	**CL_24h**	CL_24h_1	Primary T cells, *Mus musculus*	CL	24 h	RNA-seq
T14		CL_24h_2				-
T15		CL_24h_3				-
T16	**RPM_24h**	RPM_24h_1	Primary T cells, *Mus musculus*	RPM	24 h	RNA-seq
T17		RPM_24h_2				-
T18		RPM_24h_3				-
J1	**HS_8h**	HS_8h_1J	Jurkat T cells, *Homo sapiens*	HS	8 h	RT-qPCR
J2		HS_8h_2J				RT-qPCR
J3		HS_8h_3J				-
J4	**CL_8h**	CL_8h_1J	Jurkat T cells, *Homo sapiens*	CL	8 h	RT-qPCR
J5		CL_8h_2J				RT-qPCR
J6		CL_8h_3J				-
J7	**RPM_8h**	RPM_8h_1J	Jurkat T cells, *Homo sapiens*	RPM	8 h	RT-qPCR
J8		RPM_8h_2J				RT-qPCR
J9		RPM_8h_3J				-
J10	**NTC_8h**	NTC_8h_1J	Jurkat T cells, *Homo sapiens*	NTC	8 h	RT-qPCR
J11		NTC_8h_2J				RT-qPCR
J12		NTC_8h_3J				-
J13	**HS_24h**	HS_24h_1J	Jurkat T cells, *Homo sapiens*	HS	24 h	RT-qPCR
J14		HS_24h_2J				RT-qPCR
J15		HS_24h_3J				-
J16	**CL_24h**	CL_24h_1J	Jurkat T cells, *Homo sapiens*	CL	24 h	RT-qPCR
J17		CL_24h_2J				RT-qPCR
J18		CL_24h_3J				-
J19	**RPM_24h**	RPM_24h_1J	Jurkat T cells, *Homo sapiens*	RPM	24 h	RT-qPCR
J20		RPM_24h_2J				RT-qPCR
J21		RPM_24h_3J				-
J22	**NTC_24h**	NTC_24h_1J	Jurkat T cells, *Homo sapiens*	NTC	24 h	RT-qPCR
J23		NTC_24h_2J				RT-qPCR
J24		NTC_24h_3J				-

Table A8. List of software used for RNA-seq data analysis.

Analysis	Software	Version	Parameters	Remarks
Mapping to reference genome	HISAT2	V2.0.5	default parameters	
Quantification	HTSeq	v0.6.1	-m union	
Differential Expression Analysis	DEGseq	v1.36.1	$\lvert \log_2 \text{Fold change} \rvert > 1$; Padj < 0.005	
	DESeq2	v1.22.2	Padj < 0.05	
GO Enrichment	GOSeq, topGO, hmmscan	v1.34.1	Padj < 0.05	padj < 0.05 were considered significantly enriched

References

1. Rich, R.R.; Fleisher, T.A.; Shearer, W.T. *Clinical Immunology: Principles and Practice*, 4th ed.; Saunders: Philadelphia, PA, USA, 2012.
2. Ullrich, O.; Thiel, C.S. Gravitational force: Triggered stress in cells of the immune system. In *Stress Challenges and Immunity in Space: From Mechanisms to Monitoring and Preventive Strategies*; Springer: Berlin/Heidelberg, Germany, 2012.
3. Tauber, S.; Hauschild, S.; Paulsen, K.; Gutewort, A.; Raig, C.; Hürlimann, E.; Biskup, J.; Philpot, C.; Lier, H.; Engelmann, F.; et al. Signal transduction in primary human T lymphocytes in altered gravity during parabolic flight and clinostat experiments. *Cell. Physiol. Biochem.* **2015**, *35*, 1034–1051. [CrossRef] [PubMed]
4. Cogoli-Greuter, M. Influence of microgravity on mitogen binding, motility and cytoskeleton patterns of T lymphocytes and jurkat cells-experiments on sounding rockets. *Jpn. J. Aerosp. Environ. Med.* **1998**, *35*, 27–39.
5. Luo, H.; Wang, C.; Feng, M.; Zhao, Y. Microgravity inhibits resting T cell immunity in an exposure time-dependent manner. *Int. J. Med. Sci.* **2013**, *11*, 87–96. [CrossRef]
6. Maccarrone, M.; Battista, N.; Meloni, M.; Bari, M.; Galleri, G.; Pippia, P.; Cogoli, A.; Finazzi-Agrò, A. Creating conditions similar to those that occur during exposure of cells to microgravity induces apoptosis in human lymphocytes by 5-lipoxygenase-mediated mitochondrial uncoupling and cytochrome c release. *J. Leukoc. Biol.* **2003**, *73*, 472–481. [CrossRef]
7. Hashemi, B.B.; Penkala, J.E.; Vens, C.; Huls, H.; Cubbage, M.; Sams, C.F. T cell activation responses are differentially regulated during clinorotation and in spaceflight. *FASEB J.* **1999**, *13*, 2071–2082. [CrossRef] [PubMed]
8. Hughes-Fulford, M.; Sugano, E.; Schopper, T.; Li, C.; Boonyaratanakornkit, J.; Cogoli, A. Early immune response and regulation of IL-2 receptor subunits. *Cell. Signal.* **2005**, *17*, 1111–1124. [CrossRef] [PubMed]
9. Lewis, M.L.; Cubano, L.A.; Zhao, B.; Dinh, H.-K.; Pabalan, J.G.; Piepmeier, E.H.; Bowman, P.D. cDNA microarray reveals altered cytoskeletal gene expression in space-flown leukemic T lymphocytes (Jurkat). *FASEB J.* **2001**, *15*, 1783–1785. [CrossRef]
10. Chang, T.T.; Walther, I.; Li, C.-F.; Boonyaratanakornkit, J.; Galleri, G.; Meloni, M.A.; Pippia, P.; Cogoli, A.; Hughes-Fulford, M. The Rel/NF-κB pathway and transcription of immediate early genes in T cell activation are inhibited by microgravity. *J. Leukoc. Biol.* **2012**, *92*, 1133–1145. [CrossRef]
11. Sonnenfeld, G. Space flight modifies T cell activation-role of microgravity. *J. Leukoc. Biol.* **2012**, *92*, 1125–1126. [CrossRef]
12. Boonyaratanakornkit, J.B.; Cogoli, A.; Li, C.-F.; Schopper, T.; Pippia, P.; Galleri, G.; Meloni, M.A.; Hughes-Fulford, M. Key gravity-sensitive signaling pathways drive T-cell activation. *FASEB J.* **2005**, *19*, 2020–2022. [CrossRef]
13. Reed, F.; Larsuel, S.T.; Mayday, M.Y.; Scanlon, V.; Krause, D.S. MRTFA: A critical protein in normal and malignant hematopoiesis and beyond. *J. Biol. Chem.* **2021**, *296*, 100543. [CrossRef] [PubMed]
14. Miranda, M.; Lichner, Z.; Szászi, K.; Kapus, A. MRTF: Basic Biology and Role in Kidney Disease. *Int. J. Mol. Sci.* **2021**, *22*, 6040. [CrossRef] [PubMed]
15. Record, J.; Sendel, A.; Kritikou, J.S.; Kuznetsov, N.V.; Brauner, H.; He, M.; Nagy, N.; Oliveira, M.; Griseti, E.; Haase, C.B.; et al. An intronic deletion in megakaryoblastic leukemia 1 is associated with hyperproliferation of B cells in triplets with Hodgkin lymphoma. *Haematologica* **2020**, *105*, 1339–1350. [CrossRef] [PubMed]
16. Herranz, R.; Anken, R.; Boonstra, J.; Braun, M.; Christianen, P.C.M.; De Geest, M.; Hauslage, J.; Hilbig, R.; Hill, R.J.A.; Lebert, M.; et al. Ground-based facilities for simulation of microgravity: Organism-specific recommendations for their use, and recommended terminology. *Astrobiology* **2013**, *13*, 1–17. [CrossRef]
17. Wuest, S.L.; Richard, S.; Kopp, S.; Grimm, D.; Egli, M. Simulated Microgravity: Critical Review on the Use of Random Positioning Machines for Mammalian Cell Culture. *BioMed Res. Int.* **2015**, *2015*, 971474. [CrossRef]
18. Brungs, S.; Hauslage, J.; Hemmersbach, R. Validation of Random Positioning Versus Clinorotation Using a Macrophage Model System. *Microgravity Sci. Technol.* **2019**, *31*, 223–230. [CrossRef]

19. Kuznetsov, N.V.; Almuzzaini, B.; Kritikou, J.S.; Baptista, M.A.P.; Oliveira, M.M.S.; Keszei, M.; Snapper, S.B.; Percipalle, P.; Westerberg, L.S. Nuclear Wiskott-Aldrich syndrome protein co-regulates T cell factor 1-mediated transcription in T cells. *Genome Med.* **2017**, *9*, 91. [CrossRef]
20. Young, M.D.; Wakefield, M.J.; Smyth, G.K.; Oshlack, A. Gene ontology analysis for RNA-seq: Accounting for selection bias. *Genome Biol.* **2010**, *11*, R14. [CrossRef]
21. Anders, S.; Huber, W. Differential expression analysis for sequence count data. *Genome Biol.* **2010**, *11*, R106. [CrossRef]
22. Anders, S.; Huber, W. Differential expression of RNA-Seq data at the gene level–the DESeq package. In *DESq Manual*; European Molecular Biology Laboratory: Heidelberg, Germany, 2012.
23. Wang, L.; Feng, Z.; Wang, X.; Wang, X.; Zhang, X. DEGseq: An R package for identifying differentially expressed genes from RNA-seq data. *Bioinformatics* **2009**, *26*, 136–138. [CrossRef]
24. Ghiorghi, Y.K.; Zeller, K.I.; Dang, C.; Kaminski, P.A. The c-Myc target gene Rcl (C6orf108) encodes a novel enzyme, deoxynucleoside 5′-monophosphate N-glycosidase. *J. Biol. Chem.* **2007**, *282*, 8150–8156. [CrossRef] [PubMed]
25. Garrett-Bakelman, F.E.; Darshi, M.; Green, S.J.; Gur, R.C.; Lin, L.; Macias, B.R.; McKenna, M.J.; Meydan, C.; Mishra, T.; Nasrini, J.; et al. The NASA twins study: A multidimensional analysis of a year-long human spaceflight. *Science* **2019**, *364*, eaau8650. [CrossRef] [PubMed]
26. Suzuki, J.; Imanishi, E.; Nagata, S. Exposure of phosphatidylserine by Xk related protein family members during apoptosis. *J. Biol. Chem.* **2014**, *289*, 30257–30267. [CrossRef]
27. Sun, D.; An, X.; Ji, B. TRIM34 facilitates the formation of multinucleated giant cells by enhancing cell fusion and phagocytosis in epithelial cells. *Exp. Cell Res.* **2019**, *384*, 111594. [CrossRef]
28. Huang, Y.; Zucker, B.; Zhang, S.; Elias, S.; Zhu, Y.; Chen, H.; Ding, T.; Li, Y.; Sun, Y.; Lou, J.; et al. Migrasome formation is mediated by assembly of micron-scale tetraspanin macrodomains. *Nat. Cell Biol.* **2019**, *21*, 991–1002. [CrossRef]
29. Zhang, Y.; Wang, J.; Ding, Y.; Zhang, J.; Xu, Y.; Xu, J.; Zheng, S.; Yang, H. Migrasome and Tetraspanins in Vascular Homeostasis: Concept, Present, and Future. *Front. Cell Dev. Biol.* **2020**, *8*, 438. [CrossRef] [PubMed]
30. Radons, J. The human HSP70 family of chaperones: Where do we stand? *Cell Stress Chaperones* **2016**, *21*, 379–404. [CrossRef]
31. Walline, C.C.; Deffit, S.N.; Wang, N.; Guindon, L.M.; Crotzer, V.L.; Liu, J.; Hollister, K.; Eisenlohr, L.C.; Brutkiewicz, R.R.; Kaplan, M.H.; et al. Virus-encoded ectopic CD74 enhances poxvirus vaccine efficacy. *Immunology* **2014**, *141*, 531–539. [CrossRef]
32. Adams, J.C. Roles of fascin in cell adhesion and motility. *Curr. Opin. Cell Biol.* **2004**, *16*, 590–596. [CrossRef]
33. Hashimoto, Y.; Kim, D.J.; Adams, J.C. The roles of fascins in health and disease. *J. Pathol.* **2011**, *224*, 289–300. [CrossRef]
34. Huang, J.; Liu, P.; Wang, G. Regulation of mitochondrion-associated cytosolic ribosomes by mammalian mitochondrial ribonuclease T2 (RNASET2). *J. Biol. Chem.* **2018**, *293*, 19633–19644. [CrossRef] [PubMed]
35. Dehghani-Tafti, S.; Levdikov, V.; Antson, A.A.; Bax, B.; Sanders, C.M. Structural and functional analysis of the nucleotide and DNA binding activities of the human PIF1 helicase. *Nucleic Acids Res.* **2019**, *47*, 3208–3222. [CrossRef] [PubMed]
36. Snow, B.E.; Mateyak, M.; Paderova, J.; Wakeham, A.; Iorio, C.; Zakian, V.; Squire, J.; Harrington, L. Murine Pif1 Interacts with Telomerase and Is Dispensable for Telomere Function In Vivo. *Mol. Cell. Biol.* **2007**, *27*, 1017–1026. [CrossRef] [PubMed]
37. Etienne-Manneville, S.; Hall, A. Rho GTPases in cell biology. *Nature* **2002**, *420*, 629–635. [CrossRef] [PubMed]
38. Tybulewicz, V.L. Vav-family proteins in T-cell signalling. *Curr. Opin. Immunol.* **2005**, *17*, 267–274. [CrossRef]
39. Mognol, G.P.; Carneiro, F.R.G.; Robbs, B.K.; Faget, D.V.; Viola, J.P.B. Cell cycle and apoptosis regulation by NFAT transcription factors: New roles for an old player. *Cell Death Dis.* **2016**, *7*, e2199. [CrossRef]
40. Gerasimčik, N.; He, M.; Dahlberg, C.I.M.; Kuznetsov, N.V.; Severinson, E.; Westerberg, L.S. The Small Rho GTPases Rac1 and Rac2 Are Important for T-Cell Independent Antigen Responses and for Suppressing Switching to IgG2b in Mice. *Front. Immunol.* **2017**, *8*, 1264. [CrossRef]
41. Krishnan, K.; Moens, P.D.J. Structure and functions of profilins. *Biophys. Rev.* **2009**, *1*, 71–81. [CrossRef]
42. Moore, D.; Bie, P.; Oser, H. *Biological and Medical Research in Space: An Overview of Life Sciences Research in Microgravity*; Springer: GmbH, Heidelberg, 1996.
43. Anken, R. Simulation of microgravity for studies in gravitational biology. *Curr. Biotechnol.* **2013**, *2*, 192–200. [CrossRef]
44. Borst, A.G.; Van Loon, J.J.W.A. Technology and developments for the Random Positioning Machine, RPM. *Microgravity Sci. Technol.* **2009**, *21*, 287–292. [CrossRef]
45. Pfister, G.; Toor, S.M.; Nair, V.S.; Elkord, E. An evaluation of sorter induced cell stress (SICS) on peripheral blood mononuclear cells (PBMCs) after different sort conditions—Are your sorted cells getting SICS? *J. Immunol. Methods* **2020**, *487*, 112902. [CrossRef] [PubMed]
46. Zhan, C.; Bidkhori, G.; Schwarz, H.; Malm, M.; Mebrahtu, A.; Field, R.; Sellick, C.; Hatton, D.; Varley, P.; Mardinoglu, A.; et al. Low Shear Stress Increases Recombinant Protein Production and High Shear Stress Increases Apoptosis in Human Cells. *iScience* **2020**, *23*, 101653. [CrossRef] [PubMed]
47. Sieck, J.B.; Budach, W.E.; Suemeghy, Z.; Leist, C.; Villiger, T.K.; Morbidelli, M.; Soos, M. Adaptation for survival: Phenotype and transcriptome response of CHO cells to elevated stress induced by agitation and sparging. *J. Biotechnol.* **2014**, *189*, 94–103. [CrossRef] [PubMed]
48. Sun, L.; Zborowski, M.; Moore, L.R.; Chalmers, J.J. Continuous, flow-through immunomagnetic cell sorting in a quadrupole field. *Cytometry* **1998**, *33*, 469–475. [CrossRef]

49. Kunnen, S.J.; Malas, T.B.; Semeins, C.M.; Bakker, A.D.; Peters, D.J.M. Comprehensive transcriptome analysis of fluid shear stress altered gene expression in renal epithelial cells. *J. Cell. Physiol.* **2018**, *233*, 3615–3628. [CrossRef]
50. Kutikhin, A.G.; Sinitsky, M.Y.; Yuzhalin, A.E.; Velikanova, E.A. Shear stress: An essential driver of endothelial progenitor cells. *J. Mol. Cell. Cardiol.* **2018**, *118*, 46–69. [CrossRef]
51. Molladavoodi, S.; Robichaud, M.; Wulff, D.; Gorbet, M. Corneal epithelial cells exposed to shear stress show altered cytoskeleton and migratory behaviour. *PLoS ONE* **2017**, *12*, e0178981. [CrossRef]
52. Hauslage, J.; Cevik, V.; Hemmersbach, R. *Pyrocystis noctiluca* represents an excellent bioassay for shear forces induced in ground-based microgravity simulators (clinostat and random positioning machine). *Npj Microgravity* **2017**, *3*, 12. [CrossRef]